# Strong Tunneling in the Single-Electron Transistor

P. Joyez, V. Bouchiat, D. Esteve, C. Urbina, and M. H. Devoret
*Service de Physique de l'Etat Condensé, Commissariat à l'Energie Atomique, Saclay, 91191 Gif-sur-Yvette, France*
(Received 27 January 1997)

We have investigated the suppression of single-electron charging effects in metallic single-electron transistors when the conductance of the tunnel junctions becomes larger than the conductance quantum $e^2/h$. We find that the Coulomb blockade of the conductance is progressively shifted at lower temperatures. The experimental results agree quantitatively with the available $1/T$ expansion at high temperature, and qualitatively with the predictions of an effective two-state model at low temperature, which predicts at $T = 0$ a blockade of conductance for all gate voltages. [S0031-9007(97)03849-0]

PACS numbers: 73.23.Hk, 73.20.Jc, 73.40.Gk, 85.30.Wx

Single-electron devices consist of small "island" electrodes whose charge is nearly perfectly quantized in units of $e$, but which can exchange electrons through tunnel junctions. These two seemingly contradictory requirements can be met if the tunnel conductances of the tunnel junctions are much lower than the conductance quantum $G_K = e^2/h$. In the recent years, different single-electron devices, such as single-electron transistors [1], turnstiles [2], and pumps [3,4], have been successfully operated, and their behavior is now well understood [5]. However, little is known on single-electron effects when the tunnel conductances are comparable to or greater than $G_K$. In this strong tunneling regime, one expects that quantum fluctuations of the island charges will eventually suppress single-electron effects. Indeed, such a suppression of Coulomb blockade with increasing tunneling strength has been observed in the particular case of tunnel junctions with only a few, well-transmitted channels [6,7]. In this Letter, we investigate the effect of strong tunneling in the case of metallic tunnel junctions with a large number of low-transparency channels.

For this purpose, we have measured the zero-voltage conductance of metallic single-electron transistors (SET) with moderate to large conductances. A SET consists of two series-connected tunnel junctions defining one island (see inset of Fig. 1) and of a gate electrode which electrostatically controls the current through the device. We first recall the predicted conductance within the sequential tunneling model (SM), on which our data analysis will be based. This model, relevant for weak tunneling, assumes that the number $n$ of electrons in the island is a good quantum number. It only considers tunnel transitions $n \to n \pm 1$ at the lowest order in perturbation theory, level shifts being neglected [5,8]. The SM predictions for the conductance $G$ of the SET can be expressed using a single function $g$ of reduced parameters: $G = G_0 g(n_g, E_C^0/k_BT)$, where $G_0 = 1/(G_{T1}^{-1} + G_{T2}^{-1})$ is the series tunnel conductance of the two junctions, $n_g = C_g V_g/e$ is the dimensionless gate charge, $T$ is the temperature, and $E_C^0 = e^2/2C_\Sigma$ is the bare charging energy of one excess electron on the island, $C_\Sigma = C_1 + C_2 + C_g$ being the total geometric capacitance of the island. The predictions of the model are summarized in Fig. 1, in the case of a zero-impedance electromagnetic environment for the SET. Finite impedance effects can be evaluated within the SM [9]. In our samples, they yield less than 1% conductance corrections which were taken into account in the data analysis.

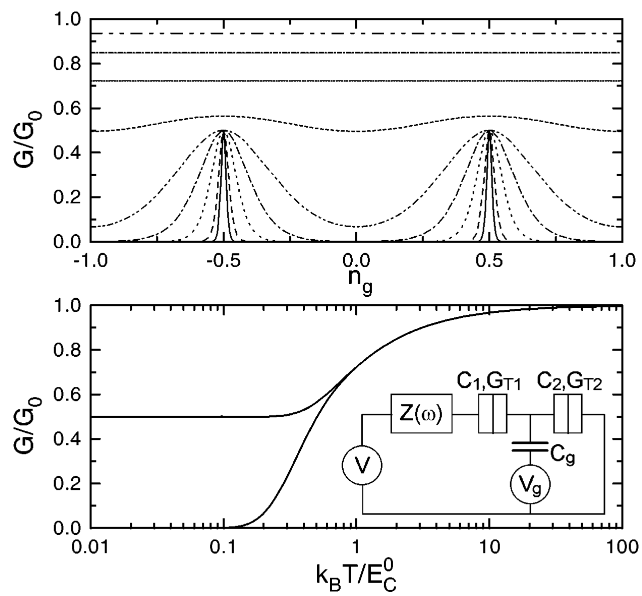


FIG. 1. Schematics of a SET and predictions of the sequential tunneling model for its conductance in the case when $Z(\omega) = 0$. Top panel: conductance of the SET as a function of the gate charge $n_g = C_g V_g/e$, for various temperatures. From top to bottom $k_BT/E_C^0 = 5$, 2, 1, 0.5, 0.2, 0.1, 0.05, 0.02, and 0.01. Bottom panel: temperature dependence of the maximum ($n_g = 1/2 \bmod 1$) and minimum ($n_g = 0 \bmod 1$) conductance. At high temperature, the conductance depends on temperature but not on $n_g$. The value $G = G_0$ is reached only in the limit $T \to \infty$. Below a certain temperature roughly given by $k_BT \approx E_C^0$, gate-charge modulation sets in and the well-known conductance peaks appear at $n_g = 1/2 \bmod 1$, for which two adjacent island charge states have the same electrostatic energy. As temperature is reduced further, the conductance peaks sharpen. The maxima remain fixed at $G/G_0 = 1/2$ and the width of the conductance peaks becomes proportional to $T$.

0031-9007/97/79(7)/1349(4)$10.00  

We now present the theoretical predictions for strong tunneling in the SET. All of them assume a zero-impedance electromagnetic environment for the SET. We define the tunneling strength parameter as $\alpha = G_{\parallel}/G_K$, where $G_{\parallel} = G_{T1} + G_{T2}$ is the parallel tunnel conductance of the two junctions. In the low temperature regime, the conductance of the SET has been calculated for arbitrary $\alpha$ [10] by mapping the system on an effective two-state model. This calculation, which only retains the lowest two electrostatic energy states of the island, is only valid near the conductance peaks and at temperatures for which the occupation of other charge states can be neglected. In the strong tunneling regime, this model predicts that the finite energy width of the island charge states prevents the conductance peaks to sharpen at low temperature, as shown in Fig. 2. Correlatively, the maximum conductance decays as $1/\ln T$ at low temperature. This suppression of conductance for all values of gate voltage is a new feature which is not predicted by weak tunneling theories. However, these predictions cannot be tested quantitatively because the model uses cutoff-dependent renormalized parameters $E_C^*$, $G_0^*$, and $\alpha^*$ [11,12] whose relation to the bare parameters is unknown in the strong tunneling regime.

At high temperatures ($k_B T \gg E_C^0$), the conductance is given by the expansion [13,14]

$$\frac{G}{G_0} = 1 - \frac{1}{3}\,\tilde{E}_C/k_B T + O[(\tilde{E}_C/k_B T)^2], \qquad (1)$$

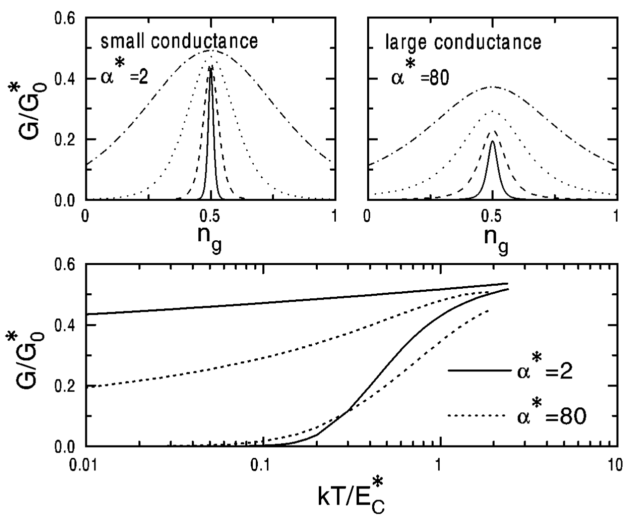


FIG. 2. Predictions of the two-state model of Ref. [10] for the reduced conductance at low temperatures. Top panels: gate-charge modulation for $k_B T/E_C^* = 0.3$, 0.1, 0.03, and 0.01 from top to bottom, respectively. Bottom panel: temperature dependence of the maximum and minimum conductance. This model, which uses renormalized parameters $E_C^*$, $G_0^*$, and $\alpha^*$, predicts a broadening of the conductance peaks and a reduction of the peak value when the tunnel conductance is increased, in qualitative agreement with the experiments (see Fig. 3). When $k_B T/E_C^*$ is of order unity or higher, the model lacks other charge states to faithfully describe the system.

where

$$\tilde{E}_C = E_C^0 \left\{ 1 - \frac{9\zeta(3)}{2\pi^4}\,\alpha\,\frac{E_C^0}{k_B T} \right\}, \qquad (2)$$

$\zeta$ being the Riemann zeta function. Expansion (1) coincides with the one found within the SM, but with $\tilde{E}_C$ in place of the bare charging energy $E_C^0$. Hence, $\tilde{E}_C$ appears as a temperature-dependent effective charging energy which contains all the effects of strong tunneling in the high temperature limit. The model developed in Ref. [14], valid for arbitrary $\alpha$, also covers the intermediate temperature range. This model is, however, not quantitative because it reproduces only part of the SM predictions and it incorporates an unknown cutoff parameter.

The samples were prepared using standard e-beam lithography and 3-angle evaporation [15] through a shadow mask [16]. The SETs were embedded in a low-pass RC electromagnetic environment necessary to the determination of $E_C^0$ in the superconducting state. The resistances consisted of 1-$\mu$m-long resistive leads made of either Cu or AuCu alloy, and were connected to on-chip 100 pF planar capacitors with one plate connected to ground. The samples were placed inside a copper shield anchored to the mixing chamber of a dilution refrigerator. Most measurements were taken in the normal state of the Al electrodes, in a 0.5 T magnetic field. The electrical wiring between the sample and the measuring apparatus at room temperature was made through filtering coaxial lines, shielded twisted pairs, and discrete miniature cryogenic filters [17]. We measured the zero-voltage conductance using a low-frequency ($\approx$10 Hz) lock-in technique, at an excitation level adjusted to probe only the linear part of the current voltage characteristic. We have investigated 4 samples, labeled 1 to 4, with increasing conductances $G_0 = 5.82$, 6.06, 24.9, and 71 $\mu$S. Assuming $G_{\parallel} = 4G_0$, since the two junctions of each sample are nominally identical, the values of $\alpha$ are 0.60, 0.62, 2.5, and 7.3, respectively. The junction size (typically $10^4$ nm$^2$) results in a number of channels of the order of $10^6$ and in a bare charging energy $E_C^0$ between 1.0 and 1.5 $k_B$K. For each sample, we measured the conductance as a function of the gate voltage $V_g$ at various temperatures. Experimental data for samples 1 and 3 are shown in Fig. 3. For sample 1 ($\alpha = 0.6$), the data closely resemble the weak tunneling predictions of the SM (see Fig. 1), as expected. In particular, the width of the peaks at low temperature scales with temperature down to 10 mK, the lowest temperature we have reached. This good electron thermalization proves the efficiency of the filtering. Deviations from the SM predictions show up in the reduction of the peak height at low temperature. We interpret this effect as a finite tunneling strength correction (the environmental resistance of the AuCu leads of this sample, of the order of 200 $\Omega$, results in a similar but much smaller effect). For sample 3 ($\alpha = 2.5$), the deviations from the SM are more pronounced: the conductance peaks are wider and the maximum conductance is more reduced at low temperature.

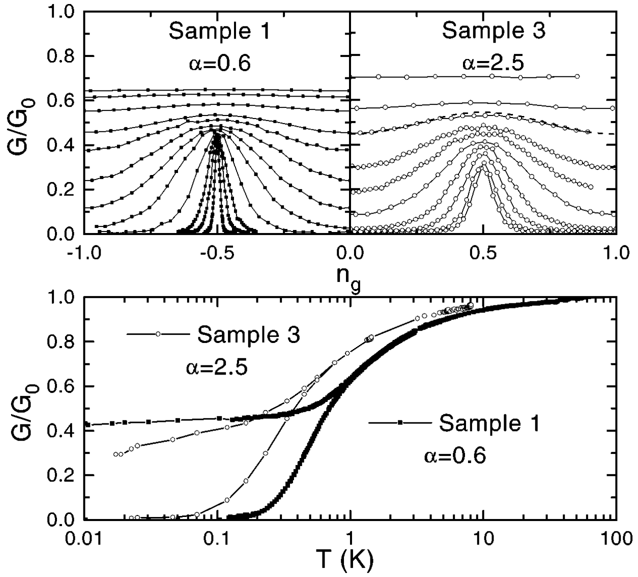


FIG. 3. Reduced measured conductance of samples 1 and 3. Top panels: variations with gate charge at various temperatures. The temperatures of the curves are, from top to bottom, 1055, 969, 796, 630, 535, 406, 303, 199, 104, 50.6, 30.5, and 10.2 mK (top left panel) and 763, 452, 335, 231, 180, 119, 70.5, 46.5, 22.8, and 17.3 mK (top right panel). The dashed line is a fit using the SM with an effective charging energy (see Fig. 4). Bottom panel: temperature dependence of the maximum and minimum conductance.

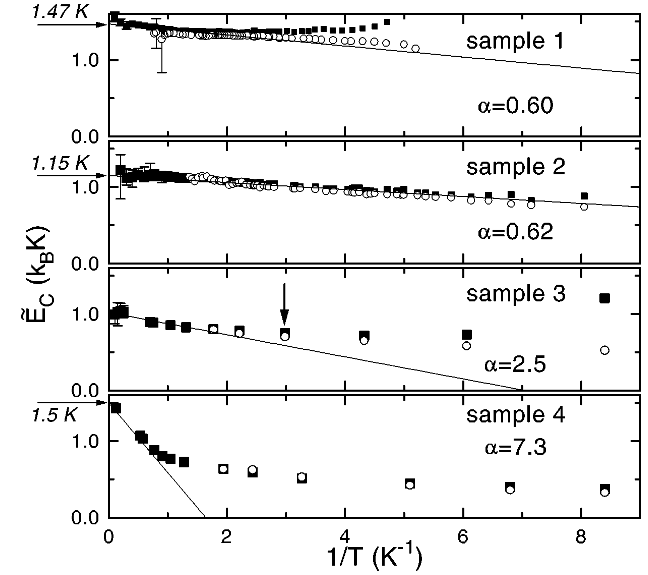


FIG. 4. For each sample, effective charging energies $\tilde{E}_{C1}$ (solid squares) and $\tilde{E}_{C2}$ (open circles) obtained from the average conductance and from the aspect ratio of the modulation, respectively (see text), and predictions of Eq. (2) (straight lines), as a function of $1/T$. The points indicated by an arrow in sample 3 correspond to the dashed curve in the top right panel of Fig. 3. Values indicated by an arrow and italic text on the left axis are the bare charging energies $E_C^0$ obtained from resonances in the superconducting state (see text and inset of Fig. 5). The predictions of Eq. (2), are calculated using the above determined $E_C^0$ for samples 1, 2, and 4, and an extrapolation for sample 3 for which the resonances could not be measured.

Note that such deviations cannot be predicted by treating quantum fluctuations as an excess temperature within the SM. The experimental results are in qualitative agreement with the predictions of the two-state model of Ref. [10], for suitably chosen $E_C^*$, $G_0^*$, and $\alpha^*$ (compare Figs. 2 and 3). Note also that the parameter $\alpha^*$ we have used is very different from the bare $\alpha$ [11].

In the high temperature regime, we have analyzed our data using the SM but with an effective charging energy as suggested by Eqs. (1) and (2). In the temperature range where there is no conductance modulation with the gate voltage, we define an effective charging energy $\tilde{E}_{C1}$ through the equation $G_{\rm exp}/G_0 = g(\tilde{E}_{C1}/k_BT)$, where $G_{\rm exp}$ is the measured conductance. In this regime, $\tilde{E}_{C1}$ is the only parameter needed to describe the data. This procedure can be generalized to the temperature range where the SET modulates, by using the $n_g$-averaged conductance, but fitting of the modulation is not guaranteed then. In this latter range, one can use a similar procedure to extract another effective energy $\tilde{E}_{C2}$ from the aspect ratio $(G_{\max} - G_{\min})/(G_{\max} + G_{\min})$ using the SM. If $\tilde{E}_{C2}$ and $\tilde{E}_{C1}$ coincide in the temperature regime where the conductance modulation is sinusoidal, the data can be well fitted using the SM with this effective charging energy. In Fig. 4, we show the values of $\tilde{E}_{C1}$ and $\tilde{E}_{C2}$ obtained following the above procedures. One finds that $\tilde{E}_{C1}$ and $\tilde{E}_{C2}$ indeed coincide in the temperature range where the modulation is sinusoidal, supporting the effective charging energy idea. The temperature dependence of the effective energies is more pronounced for increasing $\alpha$. The reduction from the $T \to \infty$ extrapolation, already noticeable for $\alpha = 0.6$, reaches 70% for $\alpha = 7.3$. This reduction can be interpreted as an increase of the effective junction capacitance, which is expected to be infinite in the limit of infinite tunnel conductance. According to Eq. (2), the $T \to \infty$ extrapolation determines the bare charging energy $E_C^0$. In order to check this prediction, we have carried out an independent determination of the charging energy $E_C^0$. For this purpose, we took advantage of the subgap resonances in the $I$-$V$ characteristic of the SET in the superconducting state. Clear observation of these resonances, due to the so-called resonant Cooper pair tunneling process [18,19], necessitates an electromagnetic environment with a smooth frequency response and sufficient dissipation, as provided by our on-chip RC circuit. These resonances are gate-voltage dependent and form a checkered pattern in a pseudo-3D $I$-$V$-$V_g$ plot, as shown in the inset of Fig. 5. From the bias voltages at which resonance crossings occur, one obtains a charging energy $E_C^S$. This charging energy differs from $E_C^0$ due to virtual electron-hole excitations. Perturbation theory at the lowest order for $n_g = 0$ yields $E_C^S = E_C^0\{1 - \alpha f(E_C^0/\Delta)\}$ where $\Delta = 180\ \mu\text{eV}$ is the gap of Al and $f(x) = \frac{x}{\pi}\int_0^{+\infty} u^2 K_{-1}^2(u) e^{-xu} du$, $K_{-1}$ being a Bessel function [20]. Using this result, one finds that $E_C^0$

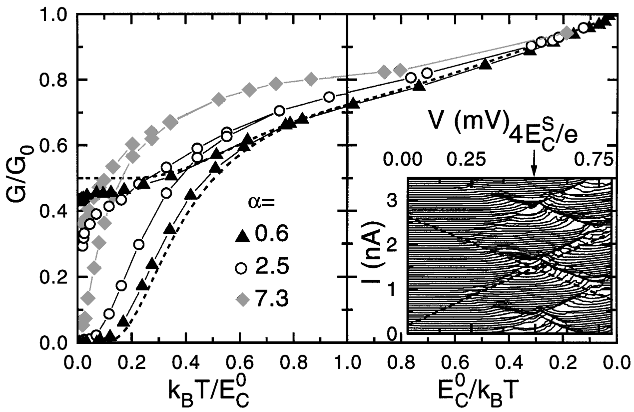


FIG. 5. Reduced conductance as a function of the reduced temperature $k_BT/E_C^0$ for samples 1 (triangles, $\alpha = 0.6$), 3 (circles, $\alpha = 2.5$), and 4 (diamonds, $\alpha = 7.3$), and predictions of the SM (dashed lines). Single-electron effects are progressively washed out as $\alpha$ increases. Inset: subgap current voltage characteristics of sample 1 taken at different $n_g$ and plotted with a vertical offset proportional to $n_g$. The checkered pattern yields a determination of the charging energy.

is 2% to 50% larger than $E_C^S$ for our samples. The values of $E_C^0$ obtained this way are indicated by arrows on the left axes in Fig. 4. Using these values, we have plotted the predictions of Eq. (2) in Fig. 4. These predictions, with no adjustable parameter, are in quantitative agreement with the experimental data in the temperature range for which the first order expansion in $\alpha$ is sufficient.

The following scenario for the suppression of Coulomb blockade with increasing tunneling strength now emerges from the temperature dependence of the maximum and minimum conductances as a function of the reduced temperature $k_BT/E_C^0$ shown in Fig. 5, for samples 1, 3, and 4. At high temperatures, strong tunneling tends to suppress Coulomb blockade, and to restore the bare conductance. The observed reduction of the effective charging energy with respect to the bare charging energy shifts the modulation regime below a temperature which decreases strongly as $\alpha$ increases. In the modulation regime, the conductance peaks are wide and their maximum continuously decays when the temperature decreases. Quantum fluctuations thus reduce not only the effective charging energy but also the amplitude of the relative conductance modulation with gate voltage. These effects, which impose a quantum limit to the performances of the SET, should be considered in electrometry applications. In conclusion, Coulomb blockade is washed out at large conductances, except at extremely low temperatures.

The authors are indebted to H. Grabert and H. Schoeller for useful discussions. This work was supported in part by the Bureau National de la Métrologie and EU ESPRIT Project SETTRON.

*Note added.*—Since our paper was submitted, König *et al.* [J. König, H. Schoeller, and G. Schön, Phys. Rev. Lett. **78**, 4482 (1997)] have proposed a new theory which covers the intermediate tunneling strength regime. Their predictions are in good agreement with our data for samples 1–3.

[1] T.A. Fulton and G.J. Dolan, Phys. Rev. Lett. **59**, 109 (1987).
[2] L.J. Geerligs, V.F. Anderegg, P.A.M. Holweg, J.E. Mooij, H. Pothier, D. Esteve, C. Urbina, and M.H. Devoret, Phys. Rev. Lett. **64**, 2691 (1990).
[3] H. Pothier, P. Lafarge, D. Esteve, C. Urbina, and M.H. Devoret, Europhys. Lett. **17**, 249 (1992).
[4] J.M. Martinis, M. Nahum, and H.D. Jensen, Phys. Rev. Lett. **72**, 904 (1994); M.W. Keller, J.M. Martinis, N.M. Zimmerman, and A. Steinbach, Appl. Phys. Lett. **69**, 1804 (1996).
[5] *Single Charge Tunneling,* edited by H. Grabert and M.H. Devoret (Plenum, New York, 1992).
[6] C. Pasquier, U. Meirav, F.I.B. Williams, D.C. Glattli, Y. Jin, and B. Etienne, Phys. Rev. Lett. **70**, 69 (1993); C. Livermore, C.H. Crouch, R.M. Westerweld, K.L. Campman, and A.C. Gossard, Science **274**, 1332 (1996), and references therein.
[7] L.W. Molenkamp, K. Flensberg, and M. Kemerink, Phys. Rev. Lett. **75**, 4282 (1995).
[8] I.O. Kulik and R.I. Shekter, Zh. Eksp. Teor. Fiz. **68**, 623 (1975) [Sov. Phys. JETP **41**, 308 (1975)].
[9] P. Joyez and D. Esteve, Phys. Rev. B **56**, 1848 (1997).
[10] J. König, H. Schoeller, and G. Schön, Europhys. Lett. **31**, 31 (1995); H. Schoeller and G. Schön, Phys. Rev. B **50**, 18 436 (1994).
[11] H. Grabert and H. Schoeller (private communication).
[12] Renormalization of charging energy has also been considered in Ref. [7] and in X. Wang, R. Egger, and H. Grabert, Europhys. Lett. **38**, 545 (1997).
[13] X. Wang, G. Göppert, and H. Grabert, Phys. Rev. B **55**, 10 213 (1997).
[14] D.S. Golubev and A.D. Zaikin, JETP Lett. **63**, 1007 (1996).
[15] D.B. Haviland, L.S. Kuzmin, P. Delsing, K.K. Likharev, and T. Claeson, Z. Phys. B **85**, 339 (1991).
[16] G.J. Dolan and J.H. Dunsmuir, Physica (Amsterdam) **152B**, 7 (1988).
[17] D. Vion, P.F. Orfila, P. Joyez, D. Esteve, and M.H. Devoret, J. Appl. Phys. **77**, 2519 (1995).
[18] D.B. Haviland, Y. Harada, P. Delsing, C.D. Chen, and T. Claeson, Phys. Rev. Lett. **73**, 1541 (1994).
[19] A. Maassen van den Brink, L.J. Geerligs, and G. Schön, Phys. Rev. Lett. **67**, 3030 (1991).
[20] V. Bouchiat, D. Esteve, G.-L. Ingold, and P. Joyez (unpublished); H. Grabert (unpublished); V. Bouchiat, Ph.D. thesis, université Paris 6, 1997.